Online Stabilization of DC Power Distribution Systems Applying MIMO-Identification Method and Resonance-Enhanced Voltage Controller

Hessamaldin Abdollahi
Electrical Engineering Department
University of South Carolina
Columbia, South Carolina 29208
abdollh@email.sc.edu

Tomi Roinila
Department of Automation
Tampere University of Technology
Tampere, Finland
tomi.roinila@tuni.fi

Silvia Arrua
Electrical Engineering Department
University of South Carolina
Columbia, South Carolina 29208
sarrua@email.sc.edu

Enrico Santi
Electrical Engineering Department
University of South Carolina
Columbia, South Carolina 29208
santi@cec.sc.edu

Abstract: In this work a stabilization control scheme is proposed for DC power distribution systems that can adapt to frequent variations in the operating conditions of the system. The proposed control scheme takes advantage of a novel rapid multiple-input multiple-output (MIMO) impedance measurement method that allows all the system impedances to be measured simultaneously. This is unlike the conventional methods where the impedances must be measured one at a time and hence several lengthy measurement cycles are needed. To stabilize the system, an adaptive resonance-enhanced voltage controller is implemented in a source converter that gets updated in real-time based on the most recent variations in the system. The proposed control scheme is validated through experimental results.

I. Introduction

In modern DC power distribution systems (PDS), power electronics converters are being increasingly incorporated due to their high level of flexibility and efficiency. These systems are found in various applications, such as DC Microgrids, More Electric Aircrafts, and onboard power distribution systems of All-Electric Ships [1]–[4]. A single bus DC PDS consisting of a source and a load subsystem is shown in Fig. 1. Each subsystem may include several feedback-controlled converters that are designed to be standalone stable. However, the interconnection of the two subsystems may result in destabilizing interactions. In fact, in a small-signal sense, the constant power load (CPL) nature of tightly regulated load converters results in a negative incremental resistance connected to the bus [5]. Such dynamics can be analyzed using an impedance-based approach along with wideband system identification methods [6]. This is achieved by utilizing the existing converters in the interconnected system to create the required perturbations, without adding dedicated measurement hardware.

Various stability criteria are presented for stability analysis of DC systems [7], [8]. These methods are mostly based on the application of the minor-loop-gain, defined as the ratio of the source output impedance (Z_S) to the load input impedance (Z_L). There are limitations with these criteria such as dependence on how subsystems are grouped and on power flow direction, and the possibility to end up with over-conservative designs [9]. Recently, the passivity-based stability criterion (PBSC) and allowable impedance region (AIR) concept are presented for stability and performance analysis of a DC PDS [9], [10]. Unlike conventional stability criteria, PBSC and AIR are applied to the system bus impedance (Z_{bus}) which is the parallel combination of Z_S and Z_L. These methods allow an effective and design-oriented stability analysis of DC PDS using the system bus impedance, Z_{bus}. In this work PBSC and AIR are adopted for stability analysis and stabilizing controller design.

Typically, a DC PDS experiences considerable changes in its operating point. Hence, a system which is stable under one operating condition, may go unstable under a different one. An example is the DC PDS

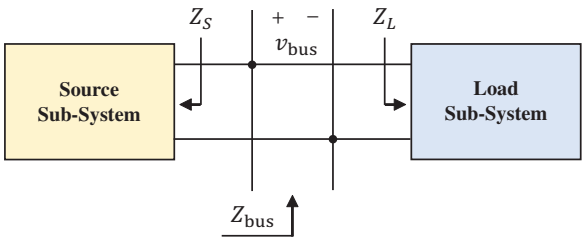

Fig. 1: A single bus DC PDS with a source subsystem and a load subsystem.

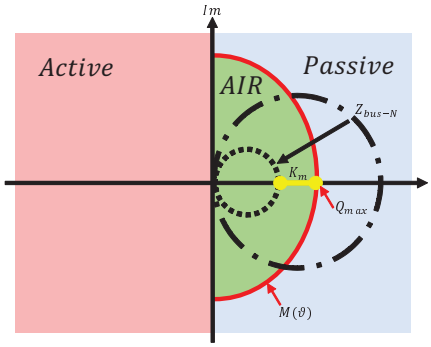

Fig. 2: PBSC requires that the Nyquist contour of Z_{bus-N} to be wholly in the right-half plane and AIR requires it to be confined within a desired region.

on the U.S. Navy All-Electric Ship, where the system configuration changes for different missions [11]. Thus, it is necessary for the control system to adapt to these changes so that stability is ensured under all operating conditions [1], [12]. A novel adaptive resonance-enhanced voltage controller, implemented in a source converter, is proposed in [13]. This adaptive controller adapts to system changes based on the measured Z_{bus}. Accordingly, Z_{bus} must be measured, which requires the measurement of the individual system impedances. A problem here is that using the conventional single-input single-output (SISO) measurement methods [14], in order to obtain the correct Z_{bus}, individual impedances must be measured one at a time. Therefore, there are challenging disadvantages: several lengthy measurement cycles are required, the measured Z_{bus} may come out corrupted because of the system operating point variations during these measurements, and additional complicating control layers are required to coordinate the injection of individual converters [15]. In this work, these problems are overcome and a stabilizing control scheme is proposed which uses a multiple-input multiple-output (MIMO) method to measure Z_{bus}. The proposed method is based on the application of orthogonal sequences and allows simultaneous measurement of all system impedances needed for the calculation of Z_{bus} [16]. The proposed stabilizing control scheme combines the advantages of the MIMO-identification method with the adaptive resonance-enhanced voltage controller to accomplish online stability analysis and performance improvement of DC PDS. This control scheme is optimized from an implementation point of view by eliminating the need for several measurement cycles, for additional coordinating control layers, and for communication channels among converters. In the proposed control algorithm: 1) all the impedances are measured simultaneously in a single cycle and Z_{bus} is calculated, 2) the stability is analyzed using PBSC and AIR, and, if needed, 3) the system is stabilized using the adaptive resonance-enhanced voltage controller.

The rest of this paper is organized as follows. Section II introduces the theoretical backgrounds with respect to PBSC and AIR, MIMO-identification method, and the adaptive resonance-enhanced controller. Section III presents the experimental results confirming the effectiveness of the presented method. Finally, Section IV draws conclusions.

II. Methods

A. PBSC and AIR

In a small-signal region around a certain operating point and in steady-state, the system shown in Fig. 1 can be considered as a linear time-invariant system. Therefore, the system stability can be analyzed using passivity-based stability criterion (PBSC) by measuring the system impedances (Z_S and Z_L) and calculating Z_{bus} as their parallel combination (see (1)).

$$\frac{1}{Z_{bus}} = \frac{1}{Z_S} + \frac{1}{Z_L} \tag{1}$$

As shown in Fig. 2, based on PBSC, which provides sufficient conditions for stability, the system is stable if Z_{bus} satisfies the passivity conditions [9]:

- $Z_{bus}(j\omega)$ contains no right-half-plane poles,
- $Re\{Z_{bus}(j\omega)\} \geq 0 \ \forall\omega$.

The second condition is equivalent to $-90° \leq arg\{Z_{bus}(j\omega)\} \leq +90° \forall\omega$ which corresponds to a network with positive resistance at all frequencies.

PBSC is a useful stability criterion that allows convenient stability analysis using the measured system bus impednace. Nevertheless, PBSC does not provide any specific information about the system dynamic performance. Therefore, to analyze the system damping level and design stabilizing controllers, the allowable impedance region (AIR) concept is developed in [10]. Typically, the bus impedance of DC PDS is dominated by a low frequency resonance [17]. So, a simplified representation of Z_{bus} can be considered as in (2).

$$Z_{bus} = Z_{o-bus} \frac{s\omega_o}{s^2 + s\omega_o/Q_{bus} + \omega_o^2} \tag{2}$$

Where Z_{o-bus} is the characteristic impedance of Z_{bus} with the resonance frequency of ω_o and the quality factor

of Q_{bus}. At the resonance frequency, Z_{bus} is equal to the product of the characteristic impedance and the quality factor, $Z_{o-bus}{*}Q_{bus}$, which is a real value. Based on the AIR concept, the bus impedance normalized by Z_{o-bus}, Z_{bus-N} given in (3), must be confined within a region in the right-half-plane bounded by $M(\theta)$ given in (4) (also see Fig. 2). In case the AIR requirement is satisfied, Z_{bus-N} is characterized by a Q which is separated from the user-specified Q_{max} by a damping margin K_m.

$$Z_{bus-N} = \frac{Z_{bus}}{Z_{o-bus}} \tag{3}$$

$$M(\theta) = Q_{max} e^{j\theta} for -\pi/2 \leq \theta \leq \pi/2 \tag{4}$$

Therefore, PBSC requirements ensure that at all frequencies the system remains passive, hence stable. Additionally, the AIR requirement guarantees that a minimum damping level is always present in the system and so a desirable dynamic performance is obtained. PBSC and AIR in combination are well suited for online stability analysis and stabilization of DC PDS and are adopted in this work.

B. MIMO Impedance Measurement Method

In a typical non-parametric frequency-response measurement of a power converter, the system input is perturbed by a pre-defined current or voltage excitation. The input and output signals are then measured, and Fourier methods are applied to extract the spectral information. Most often, a wideband perturbation such as sum of sinusoids or impulse is applied. These types of injections have energy at multiple frequencies making it possible to measure the frequency response simultaneously at several frequencies.

For linear identification of sensitive systems, a binary signal such as maximum-length pseudo-random binary sequence (MLBS) offers the best possible choice in terms of maximizing signal power within time-domain-amplitude constraints [18]. MLBS is a periodic broadband signal that has a wide controllable spectral energy distribution. Another major advantage of the MLBS, over other types of signals such as sinusoids, is that the sequence can be implemented with a low-cost shift register circuit [19].

A DC PDS is a multiple-input-multiple-output (MIMO) system. Due to cross-couplings in this MIMO system, the measurement of impedances becomes tedious using the conventional SISO technique. In this technique, to obtain system frequency responses, a perturbation signal is injected into a system input while all other inputs are zero. Subsequently, the responses are measured at all outputs in turn, and Fourier techniques are applied to each input and output signal pairs [14]. So, to measure each impedance in the system, a separate lengthy measurement cycle must be used. Also, there is the possibility that the obtained overall Z_{bus} be corrupted because of potential variations in the system operating point during these measurement cycles. Therefore, online monitoring and adaptive control of DC PDS is not easily achievable using the conventional SISO methods [2], [20], [21].

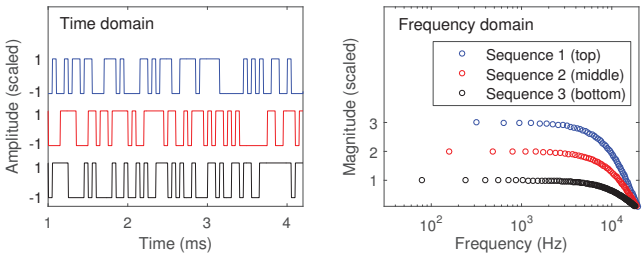

Fig. 3: Three orthogonal sequences in time and frequency domains.

An alternative to the conventional method is to apply orthogonal perturbation sequences [18]. In this method, several perturbations are simultaneously injected through system inputs. As the injections are orthogonal, that is, they have energy at different frequencies, several input-output transfer function can be measured at the same time within a single measurement cycle. This method has several substantial advantages over the conventional technique. This technique not only reduces the overall measurement time, but also ensures that each input-output transfer function is measured under the same operating condition.

The synthesis of orthogonal (periodic) binary sequences is done based on Hadamard modulation technique. In this method, the maximum-length binary sequence (MLBS) is used as the base signal. The second sequence is obtained by adding, modulo 2, the sequence 0 0 1 1 0 0... to the MLBS. The third sequence is obtained by adding the sequence 0 0 0 0 1 1 1 1 0 0 0 0... to the MLBS, and so on. Note, that the sequence length of the i^{th} orthogonal sequence is doubled compared to the length of the $(i-1)^{th}$ sequence [16], [22].

Fig. 3 shows samples of three orthogonal binary sequences in the time and frequency domain, obtained by the Hadamard modulation. The first sequence is a conventional MLBS that has 63 bits. All sequences are generated at $20kHz$. As is shown, all three signals have similar time-domain properties, but if one signal has non-zero energy at a certain frequency, the other two signals have zero energy at that frequency. Therefore, the proposed MIMO-identification method, with several unique advantages mentioned above, is used in this work to measure the system impedances and calculate the system bus impedance.

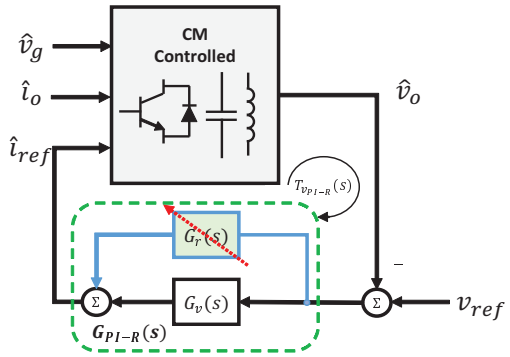

Fig. 4: Control block diagram of the source converter.

C. Adaptive Resonance-Enhanced Voltage Controller

In this work, the source is a Buck converter under two-loop control where an outer voltage loop provides reference to an inner current loop. Both the current controller and voltage controller, $G_v(s)$, are based on PI strategy with $G_v(s) = K_{p-v}+K_{i-v}/s$. The control block diagram of the system is shown in Fig. 4 where the converter block represents the model with the current loop closed. The current-mode model of the source converter is given in (5). More details on the derivation of this model can be found in [10], [13].

To ensure that PBSC and AIR are satisfied, in this work, the nominal PI voltage controller is enhanced to PI-R where the nominal controller is augmented with an adaptive resonance (R) term. This adaptive resonance term is designed and tuned so that it acts as an equivalent lossless damping impedance, Z_{damp}, which is only effective at the resonance frequency of Z_{bus-PI} and in a band around it.

$$\begin{bmatrix} \hat{i}_g \\ \hat{v}_o \\ \hat{i}_l \end{bmatrix} = \begin{bmatrix} Y_{in_c} & G_{ig-io_c} & G_{ig-c_c} \\ G_{v-g_c} & -Z_{o_c} & G_{v-c_c} \\ G_{il-ig_c} & G_{il-io_c} & G_{il-c_c} \end{bmatrix} \begin{bmatrix} \hat{v}_g \\ \hat{i}_o \\ \hat{i}_{ref} \end{bmatrix} \quad (5)$$

The modified voltage controller of the source converter, $G_{PI-R}(s) = G_v(s)+G_r(s)$, is shown in Fig. 4, and the transfer function of the additional resonance term, $G_r(s)$, is given in (6). In $G_r(s)$, ω_o, is tuned at the resonance frequency of the measured bus impedance, Z_{bus-PI}, ω_r is the bandwidth in which the controller's damping action is effective, and K_r is the peak value of $G_r(s)$.

$$G_r(s) = \frac{2K_r\omega_r s}{s^2 + 2\omega_r s + \omega_o^2} \quad (6)$$

Because of the added resonance term, the modified voltage loop-gain, $T_{v_{PI-R}}$, is increased in a frequency band around the resonance frequency. This, in turn, results in a magnitude reduction of the source output impedance in the same range. Therefore, the damping

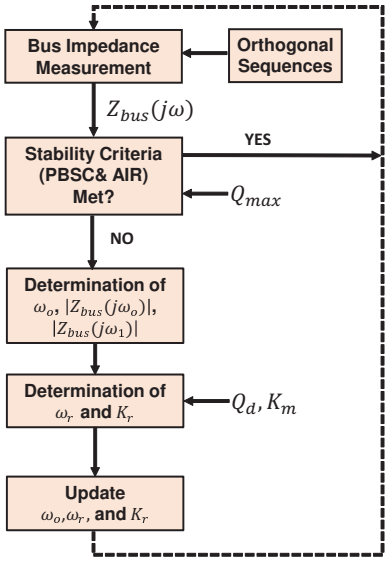

Fig. 5: The flowchart representing the proposed adaptive stabilizing control scheme.

of the source output impedance gets reflected in the bus impedance that is given in (7). In (7), Z_{bus-PI} is the bus impedance when the source converter has its output voltage regulated by the nominal PI controller. Assuming that the bandwidth of the current loop is sufficiently larger than that of the voltage loop, it can be shown that the inverse of the added resonance term appears as the desired virtual damping impedance at the bus as in (8) [13].

$$\frac{1}{Z_{bus_{PI-R}}} = \frac{1}{Z_{bus_{PI}}} + \frac{1}{Z_{damp}} \quad (7)$$

$$Z_{damp}(s) = \frac{1}{G_r(s)} \quad (8)$$

The design of the resonance-enhanced voltage controller is accomplished in two steps [13]:

- Design of the nominal PI controller, $G_v(s)$,
- Design of the adaptive resonance term, $G_r(s)$.

The design of the nominal PI part is based on the desired crossover frequency and phase-margin [23]. For the design of the resonance term, a damping impedance, given in (9), is considered which is equivalent to a series RLC impedance.

$$Z_{damp}(s) = Z_{o-damp}\frac{s^2 + s\omega_o/Q_d + \omega_o^2}{s\omega_o} \quad (9)$$

The design of $G_r(s)$ is based on the AIR concept applied to the normalized bus impedance as given in (3). It must be noted that, based on PBSC and AIR, the system must remain passive and stable with a minimum level of damping at the resonance frequency of the bus

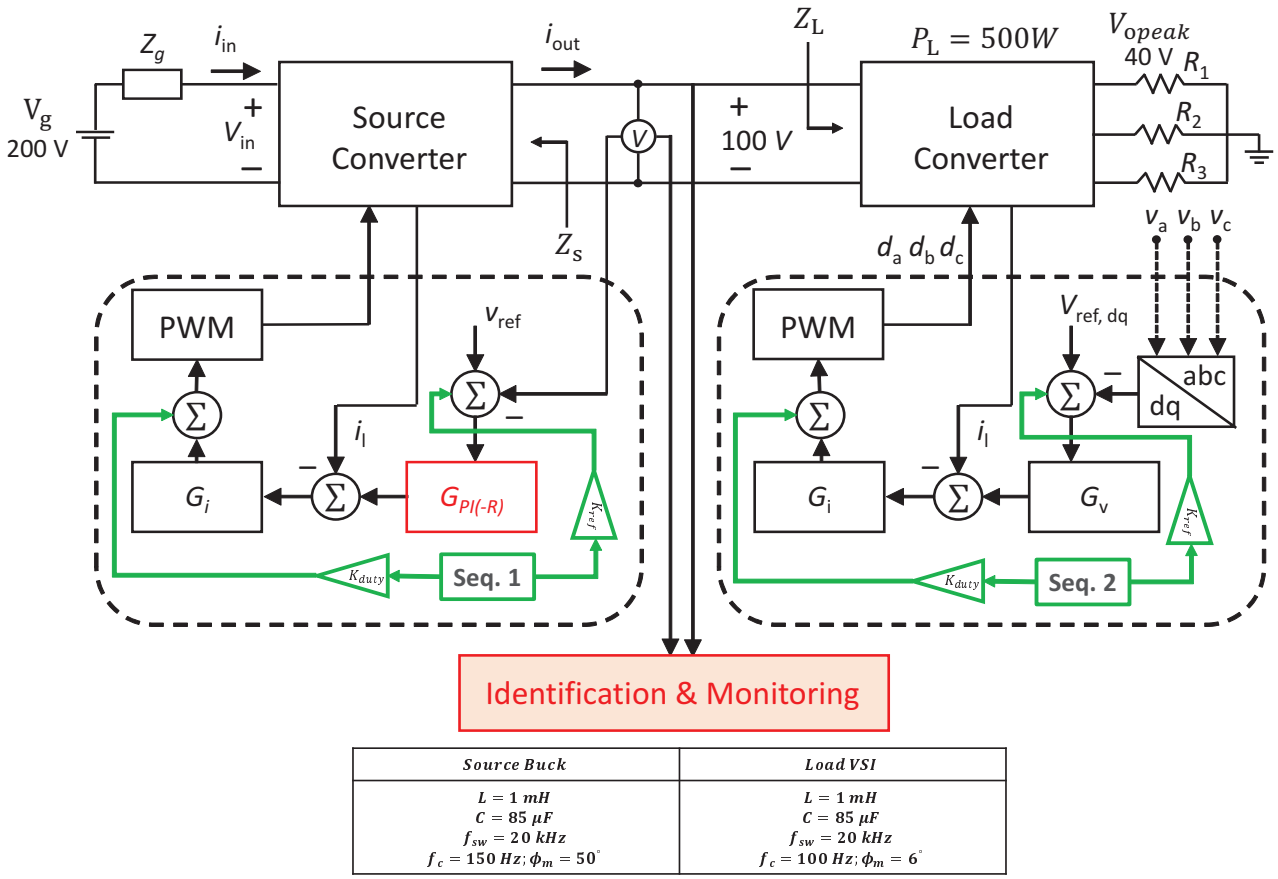

Source Buck	*Load VSI*
$L = 1\ mH$ $C = 85\ \mu F$ $f_{sw} = 20\ kHz$ $f_c = 150\ Hz; \phi_m = 50^\circ$	$L = 1\ mH$ $C = 85\ \mu F$ $f_{sw} = 20\ kHz$ $f_c = 100\ Hz; \phi_m = 6^\circ$

Fig. 6: Experimental setup used for the validation of the proposed control method.

impedance. Accordingly, the AIR requirement applied to Z_{bus-N} is formulated as in (10).

$$|Z_{bus_N}(j\omega_o)| = Q_{max} - K_m \tag{10}$$

Based on the expression of Z_{damp}, on the requirement in (10), and on the simplified bus impedance given in (2), the characteristic impedance of the damping impedance, Z_{o-damp}, is found as given in (11).

$$Z_{o-damp} = Z_{o-bus}\frac{Q_d Q_{bus}(Q_{max} - K_m)}{Q_{bus} - (Q_{max} - K_m)} \tag{11}$$

The inputs to this design procedure are Q_d, K_m, and Q_{max} which are the quality factor of Z_{damp}, the separation margin from AIR boundary, and the real-axis intersect of AIR boundary, respectively (see Fig. 2). On the other hand, $Z_{o-bus} = |Z_{bus}(j\omega_1)| * \omega_o/\omega_1$ with $\omega_1 \ll \omega_o$, and $Q_{bus} = |Z_{bus}(j\omega_o)|/Z_{o-bus}$ are found from the measured bus impedance. More details on the derivation of (11) can be found in [13]. With Z_{o-damp} obtained from (11), the virtual damping impedance design is completed and it is realized using the resonance controller, $G_r(s)$. The parameters of the resonance term, K_r and ω_r, are obtained from (6) and (9) as given in (12).

$$K_r = \frac{Q_d}{Z_{o-damp}}; \omega_r = \frac{\omega_o}{2Q_d} \tag{12}$$

The proposed MIMO method and PI-R controller are well suited for online monitoring and adaptive stabilization of DC PDS. The flowchart in Fig. 5 shows the proposed control algorithm wherein Z_{bus} is obtained in a single cycle using the MIMO method. The stability is verified based on PBSC and AIR requirements, as introduced earlier. In the case these requirements are not satisfied, the adaptive PI-R is redesigned based on the proposed design procedure and the controller gains are updated. In particular, using the measured bus impedance, the resonance frequency, ω_o, the magnitude of Z_{bus} at this frequency and ω_1, $|Z_{bus}(j\omega_o)|$ and $|Z_{bus}(j\omega_1)|$, are obtained. This information and the user specified quantities, Q_d, K_m, and Q_{max}, are then used to design and update $G_r(s)$.

Therefore, using the proposed adaptive stabilizing control scheme, the stability of DC PDS is continuously or periodically monitored and at all operating points the system stability margins and performance are preserved at a desired level.

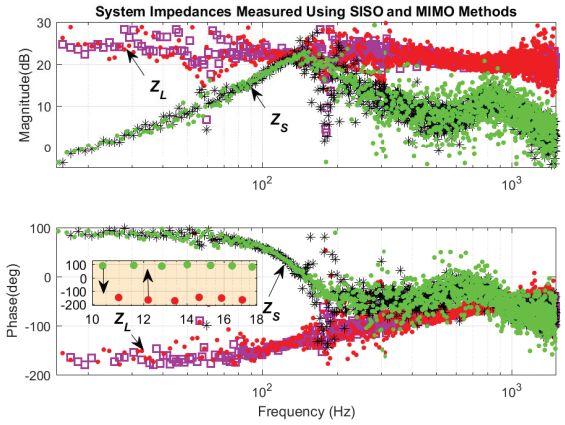

Fig. 7: System impedances measured using SISO (Z_L square and Z_S asterisk) and MIMO methods (red and green dots).

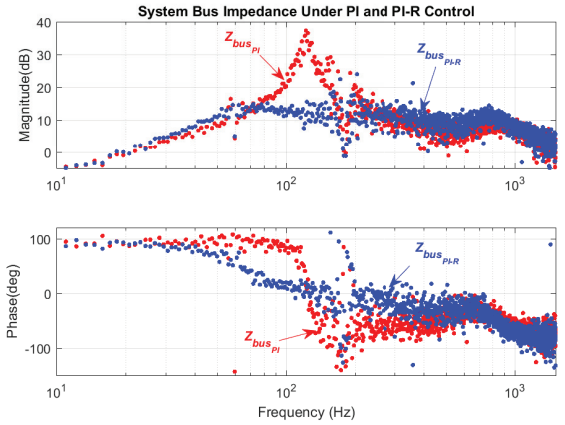

Fig. 8: Bus impedance under PI (red) and PI-R (blue) controllers.

III. Experimental Validation

The experimental validation of the proposed adaptive control scheme is presented here. The setup shown in Fig. 6 is built in the laboratory where a source Buck converter supplies a three-phase VSI load converter, both having a switching frequency of $f_{sw} = 20kHz$. The system power level is $500W$ and both converters are under two-loop PI-based control strategy implemented in a dSPACE DS1104 DSP-based control platform. Using a double-injection technique (see the Appendix), two orthogonal perturbation sequences are designed and added to the voltage reference and duty cycle signals. The sequences are scaled properly so that the injected perturbation does not exceed 5% of the nominal value of the references and duty cycles. The base MLBS is of length $N = 2^{14} - 1$ and the second sequence is of length $2N$. The sequences are generated at $f_{gen} = 20kHz$ and the sampling frequency is $f_s = 100kHz$. The impedances are found by calculating the FFT of the measured bus voltage and current and performing logarithmic averaging [24]. The system impedances, shown

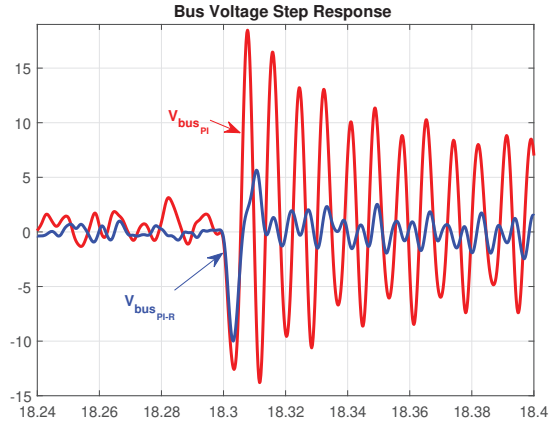

Fig. 9: The ac-coupled bus voltage response to a step change in the load VSI voltage.

in Fig. 7, with the source under PI control, are measured using both the conventional SISO and proposed MIMO methods. As can be seen, the impedances measured using the proposed MIMO method, obtained in a single measurement cycle, well match those measured using the SISO method, obtained in two separate cycles. The inset in Fig. 7 shows that the measured responses are orthogonal to each other which is the advantageous inherent property of the MIMO method. The bus impedance, $Z_{bus_{PI}}$, shown in Fig. 8, exhibits a large resonance at $f_o = 120\ Hz$. Based on PBSC the system is stable, but it is predicted to be poorly damped. This is confirmed by the (ac-coupled) bus voltage step response shown in Fig. 9: after a step variation in the load current, $V_{bus_{PI}}$ has a lightly damped oscillatory response before converging back to zero, confirming that the system is suffering from a poor damping level. Therefore, to improve the system performance and stability margins, the proposed adaptive PI-R controller is designed, using the information obtained from the measured $Z_{bus_{PI}}$, and activated at the source. For the design, $\omega_1 = 0.1\omega_o$, $Q_d = 0.5$, and $K_m = 0.3$ are chosen. The bus impedance under PI-R control, $Z_{bus_{PI-R}}$, is measured again and shown in Fig. 7. It is seen that the adaptive PI-R controller very well damps the resonant peak in $Z_{bus_{PI}}$. Also, note that due to the damping effect, the phase of $Z_{bus_{PI-R}}$ is very close to zero around the resonance frequency. The bus voltage response to the same step variation in the load current, under PI-R control, is also shown in Fig. 9. The significant improvement in the system damping level is also clear from the step response, $V_{bus_{PI-R}}$, in Fig. 9. The provided experimental results prove the effectiveness of the proposed adaptive stabilizing control algorithm.

IV. Conclusion

This work proposes a novel adaptive stabilizing control scheme for the stabilization of DC PDS using a MIMO measurement method and a resonance-enhanced voltage controller. Using the proposed method, unlike the conventional SISO method, the bus impedance can be obtained in a single measurement cycle. The stability is then analyzed based on PBSC and AIR requirements and, to stabilize the system, the adaptive PI-R controller is designed and activated in an online fashion. A design procedure for adaptive resonance-enhanced voltage controller is provided. The experimental results confirm the effectiveness of the proposed scheme in stabilizing a poorly damped single bus DC PDS.

Appendix

A. Double-injection Technique

In this work, the system impedances are measured using a double-injection technique that is briefly described in this appendix. In Fig. 6, it is shown that the perturbation sequences are scaled and added to the duty cycles and voltage references. Conventionally, the measurement is done by injecting the perturbation only into the duty cycle signal [14]. Although this may result in a fairly good high frequency measurement, the low frequency measurement quality is affected by the feedback loop. Using the double-injection technique, on the other hand, two separate, properly scaled, injections are added to duty cycle and voltage reference. In this case, the perturbation-to-output voltage transfer functions for the injections in duty cycle and voltage reference are given in (A1) and (A2), respectively. At low-frequency where the voltage loop-gain, $T_v(j\omega)$, is large in magnitude, (A1) can be approximated by $G_{vd}/T_v(j\omega)$ where G_{vd} is the duty-to-output voltage transfer function. Therefore, at low frequencies the feedback loop attenuates the injection in the duty cycle while passing through the injection into the voltage reference. At high frequency, where $T_v(j\omega)$, is small in amplitude, the opposite occurs. Hence, the procedure based on double-injection results in high quality impedance measurements in the entire frequency range of interest.

$$\left(\frac{\hat{v}}{perturbation}\right)_{duty} = \frac{G_{vd}}{1+T_v(j\omega)} \tag{A1}$$

$$\left(\frac{\hat{v}}{perturbation}\right)_{v_{ref}} = \frac{T_v(j\omega)}{1+T_v(j\omega)} \tag{A2}$$

The scaling gains (K_{ref} and K_{duty}) are chosen such that the perturbed voltage reference and duty cycle do not deviate more than $5\% - 10\%$ from their nominal values. The strength of the injection depends on the noise level and the sensitivity of the system. Too large of an injection might drive the system out of the small-signal region around a certain operating point which is not desirable.

Acknowledgment

This research was conducted under ONR grant N00014-16-1-2956 and was approved for public release under DCN# 43-5435-19.

References

[1] A. Riccobono, M. Cupelli, A. Monti, E. Santi, T. Roinila, H. Abdollahi, S. Arrua, and R. A. Dougal, "Stability of shipboard dc power distribution: Online impedance-based systems methods," *IEEE Electrification Magazine*, vol. 5, no. 3, pp. 55–67, Sept 2017.

[2] A. Khodamoradi, G. Liu, P. Mattavelli, T. Caldognetto, and P. Magnone, "Analysis of an online stability monitoring approach for dc microgrid power converters," *IEEE Transactions on Power Electronics*, vol. 34, no. 5, pp. 4794–4806, May 2019.

[3] H. Zhang, F. Mollet, C. Saudemont, and B. Robyns, "Experimental validation of energy storage system management strategies for a local dc distribution system of more electric aircraft," *IEEE Transactions on Industrial Electronics*, vol. 57, no. 12, pp. 3905–3916, Dec 2010.

[4] N. Ghanbari, M. Mobarrez, and S. Bhattacharya, "A review and modeling of different droop control based methods for battery state of the charge balancing in dc microgrids," in *IECON 2018 - 44th Annual Conference of the IEEE Industrial Electronics Society*, Oct 2018, pp. 1625–1632.

[5] A. Emadi, A. Khaligh, C. H. Rivetta, and G. A. Williamson, "Constant power loads and negative impedance instability in automotive systems: definition, modeling, stability, and control of power electronic converters and motor drives," *IEEE Transactions on Vehicular Technology*, vol. 55, no. 4, pp. 1112–1125, July 2006.

[6] E. Santi, H. Y. Cho, A. B. Barkley, D. Martin, and A. Riccobono, "Tools to address system level issues in power electronics: The digital network analyzer method and the positive feedforward control technique," in *8th International Conference on Power Electronics - ECCE Asia*, May 2011, pp. 2106–2113.

[7] R. D. D. Middlebrook, "Input filter consideration in design and application of switching regulators," in *IEEE Ind. Applicat. Soc. Annu. Meeting*, 1976, pp. 366–382.

[8] S. D. Sudhoff, S. F. Glover, P. T. Lamm, D. H. Schmucker, and D. E. Delisle, "Admittance space stability analysis of power electronic systems," *IEEE Transactions on Aerospace and Electronic Systems*, vol. 36, no. 3, pp. 965–973, Jul 2000.

[9] A. Riccobono and E. Santi, "Comprehensive review of stability criteria for dc power distribution systems," *IEEE Transactions on Industry Applications*, vol. 50, no. 5, pp. 3525–3535, Sept 2014.

[10] J. Siegers, S. Arrua, and E. Santi, "Stabilizing controller design for multibus mvdc distribution systems using a passivity-based stability criterion and positive feedforward control," *IEEE Journal of Emerging and Selected Topics in Power Electronics*, vol. 5, no. 1, pp. 14–27, March 2017.

[11] N. Doerry, "Next Generation Integrated Power Systems NGIPS Technology Development Roadmap," 2007, p. 120.

[12] S. Arrua, H. Abdollahi, and E. Santi, "Positive feed-forward control design for dc bus stabilization of a multi-converter system using a pole placement approach," in *2018 IEEE Energy Conversion Congress and Exposition (ECCE)*, Sep. 2018, pp. 4135–4140.

[13] H. Abdollahi, S. Arrua, T. Roinila, and E. Santi, "A novel dc power distribution system stabilization method based on adaptive resonance-enhanced voltage controller," *IEEE Transactions on Industrial Electronics*, pp. 1–1, 2018.

[14] A. Barkley and E. Santi, "Online monitoring of network impedances using digital network analyzer techniques," in *2009 Twenty-Fourth Annual IEEE Applied Power Electronics Conference and Exposition*, Feb 2009, pp. 440–446.

[15] T. Roinila, H. Abdollahi, S. Arrua, and E. Santi, "Online measurement of bus impedance of interconnected power electronics systems: Applying orthogonal sequences," in *2017 IEEE Energy Conversion Congress and Exposition (ECCE)*, Oct 2017, pp. 5783–5788.

[16] ——, "Real-time stability analysis and control of multi-converter systems by using mimo-identification techniques," *IEEE Transactions on Power Electronics*, pp. 1–1, 2018.

[17] S. K. Pidaparthy, B. Choi, and Y. Kim, "A load impedance specification of dc power systems for desired dc-link dynamics and reduced conservativeness," *IEEE Transactions on Power Electronics*, vol. 34, no. 2, pp. 1407–1419, Feb 2019.

[18] K. Godfrey, Ed., *Perturbation Signals for System Identification*. Hertfordshire, UK, UK: Prentice Hall International (UK) Ltd., 1993.

[19] T. Roinila, H. Abdollahi, S. Arrua, and E. Santi, "Adaptive control of dc power distribution systems: Applying pseudo-random sequences and fourier techniques," in *2018 International Power Electronics Conference (IPEC-Niigata 2018 -ECCE Asia)*, May 2018, pp. 1719–1723.

[20] ——, "Mimo identification techniques in online measurement of bus impedance of interconnected power-electronics systems," in *2017 IEEE Electric Ship Technologies Symposium (ESTS)*, Aug 2017, pp. 316–321.

[21] G. Liu, A. Khodamoradi, P. Mattavelli, T. Caldognetto, and P. Magnone, "Plug and play dc-dc converters for smart dc nanogrids with advanced control ancillary services," in *2018 IEEE 23rd International Workshop on Computer Aided Modeling and Design of Communication Links and Networks (CAMAD)*, Sep. 2018, pp. 1–6.

[22] R. Luhtala, T. Roinila, and T. Messo, "Implementation of real-time impedance-based stability assessment of grid-connected systems using mimo-identification techniques," *IEEE Transactions on Industry Applications*, pp. 5054–5063, Sep 2018.

[23] R. W. Erickson, *Fundamentals of Power Electronics*, 2002, vol. 49, no. 0.

[24] R. Pintelon and J. Schoukens, *System identification: a frequency domain approach*, 2001.